Reg Environ Change (2013) 13 (Suppl 1):S91–S100
DOI 10.1007/s10113-013-0408-8

ORIGINAL ARTICLE

Implications of multi-scale sea level and climate variability for coastal resources

A case study for south Florida and Everglades National Park, USA

Christina Karamperidou · Victor Engel · Upmanu Lall · Erik Stabenau · Thomas J. Smith III

Received: 2 August 2012 / Accepted: 13 January 2013 / Published online: 1 February 2013

Abstract While secular changes in regional sea levels and their implications for coastal zone management have been studied extensively, less attention is being paid to natural fluctuations in sea levels, whose interaction with a higher mean level could have significant impacts on low-lying areas, such as wetlands. Here, the long record of sea level at Key West, FL is studied in terms of both the secular trend and the multi-scale sea level variations. This analysis is then used to explore implications for the Everglades National Park (ENP), which is recognized internationally for its ecological significance, and is the site of the largest wetland restoration project in the world. Very shallow topographic gradients (3–6 cm per km) make the region susceptible to small changes in sea level. Observations of surface water levels from a monitoring network within ENP exhibit both the long-term trends and the interannual-to-(multi)decadal variability that are observed in the Key West record. Water levels recorded at four long-term monitoring stations within ENP exhibit increasing trends approximately equal to or larger than the long-term trend at Key West. Time- and frequency-domain analyses highlight the potential influence of climate mechanisms, such as the El Niño/Southern Oscillation and the North Atlantic Oscillation (NAO), on Key West sea levels and marsh water levels, and the potential modulation of their influence by the background state of the North Atlantic Sea Surface Temperatures. In particular, the Key West sea levels are found to be positively correlated with the NAO index, while the two series exhibit high spectral power during the transition to a cold Atlantic Multidecadal Oscillation (AMO). The correlation between the Key West sea levels and the NINO3 Index reverses its sign in coincidence with a reversal of the AMO phase. Water levels in ENP are also influenced by precipitation and freshwater releases from the northern boundary of the Park. The analysis of both climate variability and climate change in such wetlands is needed to inform management practices in coastal wetland zones around the world.

Keywords Sea level fluctuations · Key West · ENSO · NAO · AMO · Everglades National Park

C. Karamperidou (✉) · U. Lall
Earth and Environmental Engineering Department, Columbia University, 500 West 120th Street, Mudd Bldg, NY, NY 10027, USA
e-mail: ck2424@columbia.edu

V. Engel · E. Stabenau
South Florida Natural Resources Center, Everglades & Biscayne National Parks, 950 N. Krome Ave., 3rd Floor, Homestead, FL 33030, USA

Present Address:
V. Engel
U.S. Geological Survey, Southeast Ecological Science Center, 7920 NW 71st Street, Gainesville, FL 32653, USA

T. J. Smith III
U.S. Geological Survey, 600 Fourth Street South, St., Petersburg, FL 33701, USA

Introduction

Long-term trends in rising sea level associated with anthropogenic forcings threaten the integrity of coastal wetland ecosystems around the world (Nicholls et al. 2007; Titus et al. 2009). Along the coast of the Everglades National Park (ENP) in south Florida, USA (Fig. 1), salt-tolerant mangrove forests have migrated approximately 3-km inland since 1940 into historically freshwater marshes and hardwood hammocks (Craighead 1971) due to a

Fig. 1 Everglades National Park and the stations used in this study

ca. 10 cm sea level rise and reductions in water levels in the inland freshwater marshes caused by development (Ross et al. 2000).

Inter-annual to decadal-scale fluctuations in sea level are related to climate phenomena such as the El Niño/Southern Oscillation (ENSO), the Atlantic Multi-decadal Oscillation (AMO), and the North Atlantic Oscillation (NAO) through their influences on atmospheric pressure gradients and local wind stress (Maul and Hanson 1991; Wakelin et al. 2003; Bindoff et al. 2007; Bingham and Hughes 2009). These sea level fluctuations have implications for the frequency, extent, and magnitude of saltwater intrusion into coastal wetlands. Salinity values in coastal wetlands and estuaries are also affected by precipitation amounts and river discharge, which in many parts of the world exhibit similar variability due to the influence of large-scale climate patterns (Ropelewski and Halpert 1987; Dettinger and Diaz 2000; Jain and Lall 2001; van Beynen et al. 2007). Since many of the species that inhabit coastal wetlands are sensitive to salinity fluctuations (e.g. Kozlowski et al. 1991), large-scale climate features that influence the location of the fresh–saltwater mixing zones, through their effect on sea level, are important for determining the local organization and functioning of these ecosystems.

In this paper, we investigate the relationships between low-frequency climate patterns, sea levels around south

Florida, and the water levels in the expansive wetlands of ENP. Previous work by Enfield et al. (2001), Kwon et al. (2006, 2007), Kwon and Lall (2009), and Park et al. (2010) show that the variability in precipitation and sea levels in south Florida can be linked to large-scale patterns of climate variability. We first examine the relationship between sea levels recorded at Key West, FL since 1913 and large-scale climate patterns, namely ENSO, NAO, and AMO. Then, we show how such relationships are also evident in water levels recorded at coastal and inland monitoring stations in ENP since the mid-twentieth century. The work presented here highlights the modulation of water levels in coastal wetlands by interannual-to-(multi)decadal climate patterns that are manifest in sea level variability and freshwater availability, and signifies the importance of developing models for the joint influences of both factors on coastal hydrology to better manage these systems.

Data and methods

Data

The data used in this study are daily sea level data maintained by the Joint Archive of the Sea Level Center (University of Hawaii) and the National Oceanographic Data Center (NOAA) for Key West, FL (24.33°N, 81.48°W). The daily NAO index is provided by the NOAA Climate Prediction Center (CPC) and is constructed by projecting the daily 500 mb height anomalies over the Northern Hemisphere onto the loading pattern of the NAO since 1950 (for more details see Hurrell et al. (2003). The NINO3 Index, defined as the sea surface temperature (SST) anomaly in the region bounded by 90°W–150°W and 5°S–5°N, is calculated from the NOAAERSSTv3 data set, which is provided by the NOAA/OAR/ESRL PSD, Boulder, Colorado, USA, from their Web site at http://www.esrl.noaa.gov/psd/ (Smith et al. 2008). The AMO index, defined as the SST anomaly over the North Atlantic, is available from the Earth System Research Laboratory of NOAA (Enfield et al. 2001).

Wavelet analysis

The main method used in this study is wavelet transform analysis, which we briefly describe here, while we refer the reader to Torrence and Compo (1998) and Grinsted et al. (2004) for a more detailed presentation.

According to Fourier theory, a signal can be expressed as the sum of a possibly infinite series of sine and cosines, referred to as a Fourier expansion. However, a Fourier expansion has only frequency resolution and not time resolution, that is, no amplitude modulation of the signal at a given frequency is considered. Moving-window Fourier transforms have been used to address this issue, but this method is sensitive to the choice of window width. Alternatively, the wavelet transform (Chui 1992; Torrence and Compo 1998) enables the identification of frequency components as well as their variation in time.

The continuous wavelet transform of a discrete sequence x_n is defined by the convolution of x_n with a scaled and translated wavelet function ψ:

$$W_n(s) = \sum_{n'=0}^{N-1} x_{n'} \psi * \left[\frac{(n'-n)\delta t}{s} \right] \tag{1}$$

where the (∗) indicates the complex conjugate, n is a localized time index, $s \neq 0$ is the scale parameter, and N is the number of points in the time series. In this study, we use the Morlet wavelet function, defined as $\psi(\eta) = \pi^{-1/4} e^{i\omega_0 t} e^{-\eta^2/2}$, where ω_0 is a frequency and η is a non-dimensional "time" parameter. By varying the wavelet scale s and translating along the localized time index n, one can construct a picture showing both the amplitude of the spectral features versus the scale and how this amplitude varies with time (e.g. Figs. 2, 4 of this study show the time variation of the cross-wavelet power versus the scale, n is on the abscissa, s is on the ordinate, and $W_n(s)$ is represented by contours).

The continuous wavelet transform is estimated by an N-times convolution of function 1 for each scale, where N is the number of points in the time series (Kaiser 1994). The numerical estimation of the wavelet power spectrum can be done using a discrete Fourier transform x_n (Torrence and Compo 1998):

$$\hat{x}_j = \frac{1}{N} \sum_{n=0}^{N-1} x_n \exp(-2\pi i j n/N) \tag{2}$$

where $j = 0, \ldots, N-1$ is the frequency index. In the continuous limit, the Fourier transform of a function $\psi(t/s)$ is given by $\bar{\psi}(s\omega)$. By the convolution theorem, the wavelet transform is the inverse Fourier transform of the product:

$$W_n(s) = \sum_{j=0}^{N-1} \bar{x}_j \bar{\psi} * (s\omega_j) \exp(i\omega_j n \delta_t). \tag{3}$$

Because the wavelet function ψ(η) is in general complex, the wavelet transform $W_n(s)$ is also complex, and the wavelet power spectrum can be defined as $|W_n(s)|^2$. For a white-noise process, the expectation value for the wavelet transform is $|W_n(s)|^2 = \sigma^2$ at all n and s.

A vertical slice through a wavelet plot is a measure of the local spectrum. The time-averaged wavelet spectrum over all the local wavelet spectra gives the global wavelet spectrum (e.g. Fig. 2a of this study):

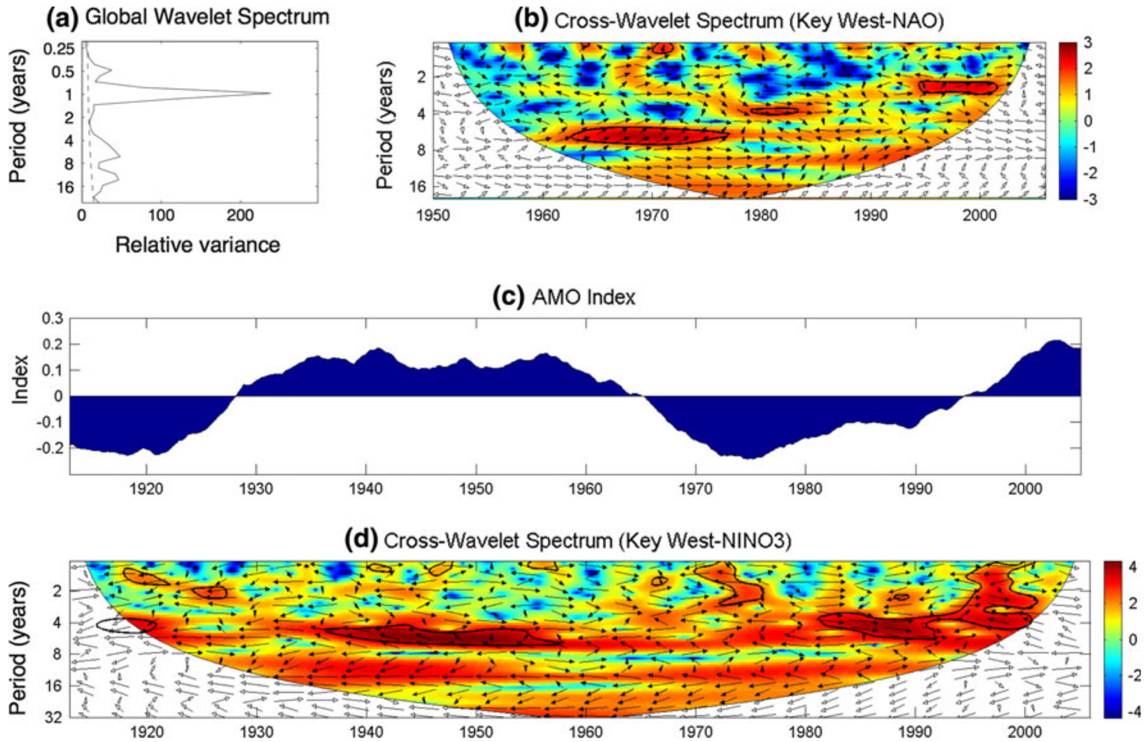

Fig. 2 **a** Global Wavelet Spectrum of the daily Key West sea level anomalies, **b** cross-wavelet power spectrum between the monthly sea level anomalies and the NAO Index, **c** AMO Index, **d** Cross-wavelet spectrum between the monthly sea level anomalies and the NINO3 Index. The *dashed line* in subplot **a**, and the *black curves* in subplots **b** and **d** indicate significance with respect to signals being AR1 processes, and the cone of influence excludes regions subject to edge effects. *Inset arrows* in the cross-wavelet plot show the relative phasing of the two time series, with *arrows* pointing to the (left)right denoting (anti)correlation

$$\bar{W}_n^2(s) = \frac{1}{N}\sum_{n=0}^{N-1} |W_n(s)|^2, \tag{4}$$

Given two time series X and Y, with wavelet transforms $W_n^X(s)$ and $W_n^Y(s)$, one can define the cross-wavelet spectrum as $W_n^{XY}(s) = W_n^X(s)W_n^{Y*}(s)$, where $W_n^{Y*}(s)$ is the complex conjugate of $W_n^Y(s)$. The cross-wavelet spectrum is complex, and hence one can define the cross-wavelet power as $W_n^{XY}(s)$. Confidence levels for the cross-wavelet power can estimated using Monte Carlo methods: A large number of surrogate data set pairs with the same AR1 coefficients as series X and Y is generated, and their cross-wavelet power is calculated. The significance levels for each scale is then estimated from this large set of surrogate data (Torrence and Compo 1998; Grinsted et al. 2004). Figures 2 and 4 of this study show the time evolution of the cross-wavelet power versus scale for the involved signals (sea levels, water levels, NAO, and NINO3 indices), as computed using the methods of Grinsted et al. (2004). The relative phasing of the two time series is indicated by the arrows in the figures, where a right-pointing arrow denotes in-phase series, and a left-pointing arrow the opposite.

Trends and interannual variability of sea levels at Key West, FL

The linear trend in Key West sea levels over the period 1913–2008 is calculated to be 2.36 ± 0.02 mm year^{-1}, which is higher than the global mean for the twentieth century (1.8 ± 0.4 mm year^{-1}), and at the lower end of the global trend (3.1 ± 0.7 mm year^{-1}) between 1993–2005 computed using satellite data (Bindoff et al. 2007). A wavelet power spectrum calculated on the daily sea level record identifies statistically significant peaks corresponding to the seasonal and annual cycles, and a broad spectrum starting at 2 years and ending at approximately 16 years (Fig. 2a). The peak found at 7.7 years can be identified with the period reported by Ghil (2002) as that of the double-gyre North Atlantic SST oscillation, which is associated with the North Atlantic mode of variability that arises from the Gulf Stream's cycle of meandering and intensification (Speich et al. 1995; Moron et al. 1998). This spectral peak appears in global, European, and North American records and its relationship with the atmosphere and the thermohaline circulation needs further investigation (Ghil and Vautard 1991; Dettinger et al. 1995; Plaut et al. 1995).

In exploring the underlying mechanisms that generate the spectral features in Fig. 2a, we note that two mechanisms can explain sea level anomalies in south Florida: shifts in northeasterly wind forcing and changing transport of the Florida Current (FC)/Gulf Stream (NOAA 2009). High northeasterly winds result in rising sea levels due to Ekman-driven convergence along the coast. Low Florida Current (FC) transport also results in high coastal sea levels because it relaxes the eastward-rising cross-current slope (Fofonoff 1980). Baringer and Larsen (2001) indicate that these two mechanisms are anti-correlated with the NAO with a lag time of approximately 18 months, while DiNezio et al. (2009) show that such an anti-correlation between the FC and the NAO may be explained by wind stress curl anomalies. More specifically, DiNezio et al. (2009) showed that the basin-wide anti-cyclonic atmospheric circulation within the circle of action of the NAO generates negative anomalies in westerly wind fields in the band 30°–40°N, and a resulting positive wind stress curl anomaly over the 20°–30°N latitudinal band of the Straits of Florida; the latter produces negative FC anomalies, thus explaining the anti-correlation between NAO and FC transport.

The influence of the NAO on Key West sea level anomalies appears to be modified with respect to the magnitude of the SST anomalies in the North Atlantic, as described by the AMO Index. Figure 2b shows the cross-wavelet spectrum between the Key West monthly record and the NAO Index, while Fig. 2c shows the historical AMO Index. In all cross-wavelet analyses, the annual cycle has been removed. Inset arrows in the cross-wavelet plot show the relative phasing of the two time series, with arrows pointing to the (left)right denoting (anti)correlation. Key West water levels and the NAO Index are positively correlated and jointly exhibit high power at periods of 6–8 years during the post-1965 transition to a strongly negative (cold) AMO phase. During cold AMO phases, the North Atlantic SSTs are below-average and are associated with areas of high atmospheric pressure that produce comparatively strong wind fields over the North Atlantic, similar to those observed during a positive NAO. This strengthening of the mean wind field over the North Atlantic about the center of action of the NAO (40°–50°N) and the associated weakening of westerlies in the band 30°–40°N and resultant weakening of the wind stress curl (see DiNezio et al. 2009) leads to negative FC transport anomalies and, consequently, higher Key West sea levels. We therefore hypothesize that the increase in power in the cross-wavelet spectrum during the cold AMO phase can be attributed to an enhancement of the general effect of the NAO positive phase on the Key West sea levels. We also note high cross-wavelet power at the 3-years period during the shift to a warm AMO phase (1995–2000); however, a hypothesis for this observation is challenging. This highlights the need for such mechanisms to be investigated through ocean and coupled ocean–atmosphere model simulations as a step toward developing coastal zone management strategies in relation to climate and sea level variability.

The cross-wavelet spectrum between Key West sea levels and the NINO3 Index reveals high power at periods of 4–7 years during the 1930–1965 AMO warm phase (Fig. 2d). The power in this band decreases to non-significant levels when the AMO shifts to a strong cold phase. The phase arrows show that the two series are in opposite phase during warm AMO, with NINO3 leading Key West. When AMO is in its post-1980 cold phase, Key West water levels and the NINO3 index are in phase and jointly exhibit high power at periods of approximately 4–7 years. The reversal of the correlation sign appears again post 1995, coinciding with a reversal of the AMO index to positive values. Direct correlation analyses (not shown here) confirm the sign change. Park et al. (2010) report that during warm AMO, the amplitudes and variance of extreme sea level events at Key West are greater than those observed during cold AMO. The negative correlation between NINO3 and Key West sea levels during warm AMO that we report here results in lower minimum Key West sea levels during warm ENSO events, which could be one component of the greater variance reported by Park et al. (2010). Kennedy et al. (2007) associate interannual variability in upper and lower daily extreme sea levels along the Gulf of Mexico (not including the Florida Straits) with variability in mid-latitude storm tracks during difference phases of ENSO. The propagation of such interactions to the Florida Straits could explain our findings in the cross-wavelet spectrum. The variability in mid-latitude storm tracks during difference phases of ENSO discussed by Kennedy et al. (2007) is effectively an expression of the interaction between ENSO and NAO, given that NAO is a measure of the strength and position of the mid-latitude storm tracks (Osborn 2007). The interactions between the climate mechanisms (e.g. ENSO, NAO, and AMO) are not well understood and are still under investigation (e.g. Zhang and Delworth 2005; Timmermann et al. 2005, 2007; Sutton and Hodson 2007; te Raa et al. 2009). The time- and frequency-domain analysis presented here provides an indication of the direction and magnitude of such interactions.

Trends and variability of water levels in the ENP

Water levels in the wetlands of ENP are influenced by sea levels, direct rainfall, and the amount of freshwater entering the Park across its northern boundary. Water management operations that control the amount of freshwater deliveries to ENP reflect regional strategies designed to balance the protection of fish and wildlife with agricultural and municipal water supplies and flood control. These strategies have changed over the past several decades, with distinct periods in water level regulations: the period 1961–1965 was marked by no freshwater releases during the construction of the control structures in the northern boundary of ENP (see Fig. 1) and was followed by a period (1965–1970) of relatively high discharges (25.98 ± 36.08 m^3s^{-1}). The subsequent period from 1971 to 1990 was marked by relatively low freshwater releases (15.25 ± 19.33 m^3s^{-1}), and a return during 1991–2008 to relatively high releases (33.33 ± 38.97 m^3s^{-1}). Prevailing rainfall conditions during these periods influenced the magnitude of these releases, although the degree to which rainfall and the freshwater releases were correlated varied over time because of changing water management strategies.

Water levels recorded at four long-term monitoring stations within ENP exhibit increasing trends approximately equal to or larger than the long-term trend at Key West (Fig. 3; Table 1). Figure 3 shows sea levels at Key West and water levels at the inland monitoring stations, as well as annual precipitation and freshwater releases measured at the northern boundary of the Park. The longest records (e.g. P33) show that the trends of water levels in ENP closely match the Key West sea level trend during the periods such as the early 1960s when overland flow across the northern Park boundary was largely blocked. Since the construction of gated control structures across the northern boundary and with the advent of managed releases (shown shaded in Fig. 3), the rate at which water levels have increased at the stations close to the northern boundary (P33 and P34) exceeds the rate of increase in sea level observed at Key West. This is evident in the inset scatterplot of the rate of water level change at the stations vs. the rate at Key West, where solid dots indicate the values in the period 1953–1965 prior to the construction of the release structures, and crosses indicate the post-1965 values. Note that the trends parallel the diagonal in the absence of managed releases, indicating that the sea level change signal at Key West is propagated inland. After the construction of the release structures, the trends at the stations are independent from the Key West trend, as shown by the crosses. For example, at P34 near the northern boundary of the Park, the 9.65 mm $year^{-1}$ trend of increasing water levels is mainly due to increased freshwater releases after the 1960s. On the other hand, the relative effect of the freshwater releases is less obvious in water levels recorded at stations located further downstream, such as P35 and P37, where the trend has remained very close to the Key West trend over the period of record (2.56 and 2.27 mm $year^{-1}$, respectively).

Cross-wavelet analyses show that interannual variability and correlation with the NINO3 and the NAO indices are also apparent in the coastal and inland ENP wetland stations (Fig. 4). The periodicities of joint high wavelet power are different between the Key West (Fig. 2) and the P35 analyses (Fig. 4), which is somewhat expected due to the fact that the P35 record spans the years 1954–2005; hence, the water levels are subjected to the additional effect of scheduled freshwater releases from the northern boundary and are not allowed to freely fluctuate in response only to natural variability. However, patterns similar to the ones observed in the Key West record (Fig. 2) emerge in the P35 record (Fig. 4), including the reversal of the NINO3 and Key West phases after the 1995 shift to the warm AMO. ENSO leads to increased wintertime precipitation in south Florida (Hagemeyer and Almeida 2002), and our results

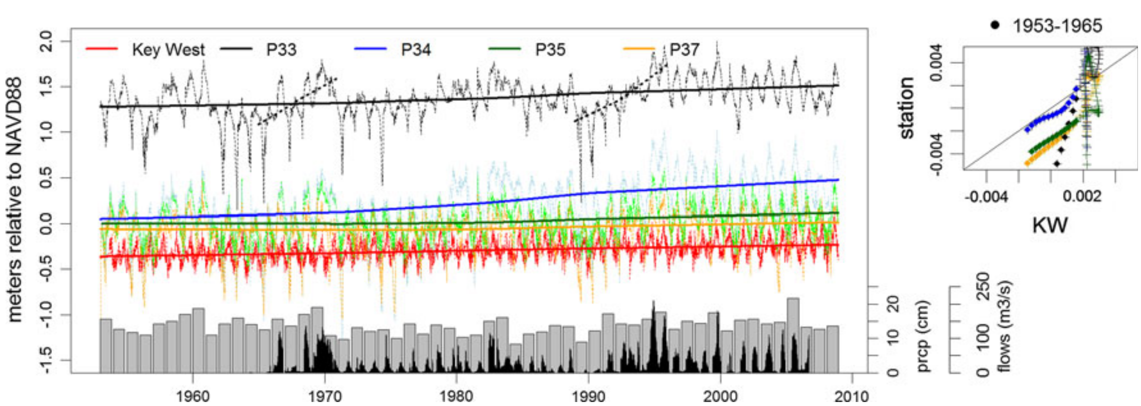

Fig. 3 The selected Park stations exhibit trends close to or higher than the Key West sea level trend. The *barplot* and *shaded areas* indicate precipitation and freshwater releases measured at the northern boundary of the Park. Short trend lines mark periods when water levels rise fast relative to the long-term trend. The *inset* figure shows the scatterplot of the rate of water level change at the stations versus the one at Key West: *solid dots mark* the values in years 1953–1965 (prior to the construction of the release structures), indicating that the trends parallel the diagonal in the absence of managed releases from the northern boundary of ENP. Crosses indicate the post-1965 values. For reasons of clarity, stations P36 and P38 are omitted

Table 1 Trends of water levels in the Park stations. Trends are calculated using the Sen's slope method (Mann 1945; Slack et al. 2003) from daily data over the period 1958–2008 for all stations, except for P36 (1968–2008). Elevation is relative to NAVD88

Station	Type	Basin	Elevation (m)	Trend (mm year^{-1})
P33	Marsh	Shark slough	1.48	4.81
P34	Marsh	East slough	0.57	9.65
P35	Marsh	Shark slough	0.25	2.56
P36	Marsh	Shark slough	0.98	8.04
P37	Marsh	Taylor slough	0.27	2.27
P38	Marsh	Shark slough	0.26	4.02
KW (Key West)	Marine	Florida keys	–	2.36

show inland water levels in ENP reflect this signal as a result of both direct rainfall and the timing and magnitude of structural releases across the northern boundary. ENSO contributes to the interannual variability in those stations further downstream and closer to the coast through its influence on both the Key West sea levels and the precipitation record, hence the high cross-wavelet power around the 4-years period in Fig. 4.

The observation of high power in the cross-wavelet spectrum of Key West sea level and the NAO Index, when the AMO changes phase, was also observed for the P35 case as indicated by the peaks in 1965 and 1995. We note a coincidence of high cross-spectral power in the periods 1965–1971 and 1985–1995, and accelerated rates of water level increase noted by the short trend lines in Fig. 3. This is attributed to the combined influence of ENSO and NAO on three of the primary factors that regulate water levels at this location, namely tidal inputs, precipitation, and managed freshwater releases at the Park's northern boundary.

Summary and discussion

While secular changes in regional sea levels and their implications for coastal zone management have been studied extensively, little attention is being paid to natural fluctuations in sea levels, whose interaction with a higher mean level could have significant impacts on ecology in low-lying areas. Here, we note the presence of secular changes, as well as natural low-frequency variability, in both coastal and inland water level fluctuations in the region of south Florida and ENP. We show that these fluctuations are linked to climate patterns, such as ENSO, NAO, and AMO; hence, improved physical understanding and modeling of these patterns and their potential interactions could benefit coastal zone management.

Our investigation into the Key West sea level record yielded the following main findings:

1. The NAO and Key West sea level anomalies are positively correlated.
2. The two series show high common power in the frequency space during the shift to cold AMO, which may be attributed to an enhancement of the general effect of the NAO positive phase on the Key West sea levels during below-average North Atlantic SSTs (cold AMO).

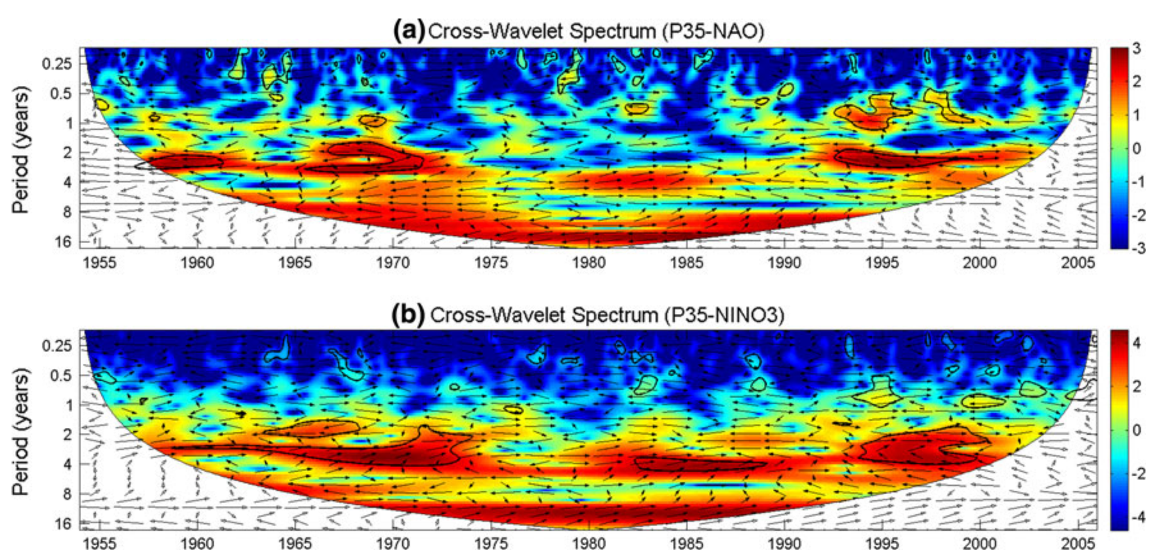

Fig. 4 Cross-wavelet power spectrum between P35 water levels and **a** the NAO Index, and **b** the NINO3 Index. *Inset arrows* in the cross-wavelet plot show the relative phasing of the two time series, with *arrows* pointing to the (left)right denoting (anti)correlation. Note the similarity in cross-wavelet power patterns (reversal of correlation sign, high power at the reversal of AMO phase etc) with the relationship between Key West levels and the NAO and NINO3 indices (compare with Fig. 2, see text for discussion)

3. ENSO and Key West sea level anomalies are not phase locked; changes in their correlation sign coincide with shifts of the AMO phase.

We then explored the variability of freshwater levels in ENP; our main findings are summarized as follows:

1. In the absence of managed freshwater releases from the northern boundary, the trends of water levels in ENP closely match the Key West sea level trend.
2. With the advent of managed releases at the northern boundary of ENP, the rate at which water levels have increased at the stations close to the northern boundary exceeds the rate of increase in sea level observed at Key West.
3. In the frequency domain, similar patterns to the ones observed for Key West were found for ENP stations, including high power during shifts of the AMO phase.
4. High cross-spectral power between the NAO and ENP water levels coincides with 5- to 10-year periods of accelerated rates of water level increase at ENP stations.

The work presented in this paper highlights the modulation of water levels in coastal wetlands by interannual-to-(multi)decadal climate patterns. Continued work is needed to ascertain the robustness of, and strengthen our understanding of these relationships through regional and global climate models, which should include extending these models to investigate the joint influences of climate factors on coastal hydrology.

Along with water levels, salinity along the ENP coast has been increasing over the past hundred years (Brewster-Wingard and Ishman 1999; Marshall et al. 2009). Targeted freshwater discharges have been cited as a possible strategy for mitigating the potential negative impacts of rising sea level and saltwater intrusion on coastal freshwater wetlands in ENP and in other areas around the world (Nicholls et al. 2007). Our results show that large-scale climate features can affect both the rate and frequency of sea level anomalies (and therefore salinity intrusion) and that their concurrent influence on interannual-to-decadal-scale variability in precipitation must be considered when forecasting ecosystem trajectories, or in developing coastal management plans. For example, Kwon and Lall (2009) introduced a hierarchical stochastic modeling system of daily precipitation in south Florida conditioned on ENSO and AMO variables. Our present analysis and ongoing research illustrate the need to develop similar multi-level statistical models of sea levels in south Florida: these models can utilize NAO and ENSO variables as predictors, with their influence varying depending on the state of the AMO, therefore incorporating the relationships shown in this study. The precipitation and sea level models described above can be combined to produce scenarios of freshwater and salinity levels in ENP, which can directly inform water and ecosystem management plans. For instance, water levels at the ENP stations used in this study have been used to predict foraging wading bird populations under different management scenarios (Kwon et al. 2011). Our ongoing research aims to directly inform such ecological models by providing projections of water levels at the ENP stations conditioned on ENSO, NAO, and AMO states.

To further illustrate the applicability of our results to the complex issue of hydrological restoration of ENP, we note that increasing or restoring freshwater discharges to ENP to match historic levels has been proposed (CERP 2005), and may help lower coastal salinities in this period of sea level rise. To be effective in reducing salinities, these discharge events may also result in larger magnitude and more persistent deep water conditions in the inland marshes during periods when combinations of climatic patterns, such as NAO and ENSO, result in anomalously high water. Persistent deep water conditions that exceed natural levels will be necessary to maintain pre-development, coastal zone salinity values in a future characterized by higher sea level but may also cause unforeseen shifts in plant community types and trophic interactions in the inland marshes.

As evident from our analysis and the above discussion, the nonstationary nature of the effects of NAO and ENSO on water levels in the Park, as shown in the wavelet analysis, highlights the importance of developing models for the joint influences of both the multi-scale sea level and precipitation fluctuations that are free of the traditional assumption of statistical stationarity of hydrologic time series, as was discussed in previous work by Jain and Lall (2001), and Milly et al. (2008). As outlined above, developing modeling schemes which can detect and discriminate between human- or climate-induced changes at multiple time scales, assess their relative effects, and produce probabilistic scenarios that utilize information from multiple sources across these time scales is especially relevant in the case of the Everglades, due to its high ecological value, and in light of the possible implications of climate variability and change for the ongoing restoration project.

Acknowledgments This work is supported by the Critical Ecosystem Studies Initiative, ENP Contract H5284-08-0003. CK was also partially supported by the Alexander S. Onassis Public Benefit Foundation Scholarship Program. TJSIII was supported by the USGS Ecosystems and GEPES programs. We thank Y. Kushnir and M. Cane for enlightening discussions. Many thanks are due to P. DiNezio for suggestions that significantly improved this manuscript, and to C. Alarcon for GIS support. Any use of trade, product, or firm names is for descriptive purposes only and does not imply endorsement by the U.S. Government.

References

Baringer M, Larsen J (2001) Sixteen years of Florida current transport at 27N. Geophys Res Lett 28(16):3179–3182

van Beynen P, Asmerom Y, Polyak V, Soto L, Polk JS (2007) Variable intensity of teleconnections during the late Holocene in subtropical North America from an isotopic study of speleothem from Florida. Geophys Res Lett 34. doi:10.1029/2007GL031046

Bingham R, Hughes C (2009) The signature of the Atlantic meridional overturning circulation in sea level along the east coast of North America. Geophys Res Lett 36. doi: 10.1029/2008GL036215

Brewster-Wingard G, Ishman S (1999) Historical trends in salinity and substrate in central and northern Florida Bay: a paleoecological reconstruction using modern analogue data. Estuaries 22(2):369–383

CERP (2005) The comprehensive everglades restoration plan. Report to congress. Available at [http://www.evergladesplan.org/]

Chui C (1992) An introduction to wavelets, wavelet analysis and its application, vol 1. Elsevier, New York

Craighead F (1971) The trees of South Florida. University of Miami Press, Coral Gables

Dettinger M, Diaz H (2000) Global characteristics of stream flow seasonality and variability. J Hydrometeorol 1:289–310

Dettinger M, Ghil M, Kepenne C (1995) Interannual and interdecadal variability in United States surface-air temperatures, 1910–1987. Clim Change 31:33–36

Di Nezio P, Gramer L, Johns W, Meinen C, Baringer M (2009) Observed interannual variability of the Florida current: wind forcing and the North Atlantic oscillation. J Phys Oceanogr 39:721–736

Enfield D, nez AMN, Trimble P (2001) The Atlantic multidecadal oscillation and its relationship to rainfall and river flows in the continental US. Geophys Res Lett 28:2077–2080

Fofonoff N (1980) The gulf stream system. In: Warren B, Wunsch C (eds.) Evolution of physical oceanography scientific surveys in honor of Henry Stommel, pp 112–139

Ghil M (2002) Natural climate variability. In: Munn T (eds) Encyclopaedia of Global Environmental Change. Wiley, New York, pp 544–549

Ghil M, Vautard R (1991) Interdecadal oscillations and the warming trend in global temperature time series. Nature 350:324–327

Grinsted A, Moore J, Jevrejeva S (2004) Application of the cross wavelet transform and wavelet coherence to geophysical time series. Nonlinear Proc Geophys 11:561–566

Hagemeyer B, Almeida R (2002) Experimental forecasting of dry season storminess over Florida and the Southeast United States from the ENSO signal using multiple linear regression techniques. In: Preprints, 16th conference on probability and statistics in the atmospheric sciences, American Meteorological Society, Orlando, FL

Hurrell J, Kushnir Y, Visbeck M, Ottersen G (2003) An overview of the North Atlantic Oscillation. The North Atlantic Oscillation: climate significance and environmental impact. Geophys Monogr 134–135

Jain S, Lall U (2001) Floods in a changing climate: does the past represent the future. Water Resour Res 37(12):3193–3205

Slack JR, Lorenz DL, et al. (2003) USGS library for S-PLUS for windows. Open-file report 03-357, US Geological Survey

Kaiser G (1994) A friendly guide to wavelets, vol 1. Holden-Day, San Francisco

Kennedy A, Griffin M, Morey S, Smith S, O'Brien J (2007) Effects of El Niño- Southern oscillation on sea level anomalies along the Gulf of Mexico coast. J Geophys Res 112:C05047. doi: 10.1029/2006JC003904

Kozlowski T, Kramer P, Pallardy S (1991) The physiological ecology of woody plants. Academic Press, San Diego, CA

Kwon HH, Lall U (2009) Simulation of daily rainfall scenarios with interannual and multidecadal climate cycles for South Florida. Stoch Environ Res Risk Assess. doi:10.1007/s00477-008-0270-2

Kwon HH, Lall U, Moon YI, Ahn H, Khalil A (2006) Episodic interannual climate oscillations and their influence on seasonal rainfall in the Everglades National Park. Water Resour Res 42:W11404. doi:10.1029/2006WR005017

Kwon HH, Lall U, Khalil A (2007) Stochastic simulation model for nonstationary time series using an autoregressive wavelet decomposition: applications to rainfall and temperature. Water Resour Res 43(W05407). doi:10.1029/2006WR005258

Kwon HH, Lall U, Engel V (2011) Predicting foraging wading bird populations in Everglades National Park from seasonal hydrologic statistics under different management scenarios. Water Resour Res 47(W09510). doi:10.1029/2010WR009552

Mann H (1945) Nonparametric tests against trend. Econometrica 13:245–259

Marshall C, Pielke R, Steyaert L, Willard D (2009) The impact of anthropogenic land-cover change on the Florida Peninsula sea breezes and warm season sensible weather. Mon Wea Rev 22(132):2852

Maul G, Hanson K (1991) Interannual coherence between North Atlantic atmospheric surface pressure and composite southern USA sea level. Geophys Res Lett 18(4):653–656

Milly P, Betancourt J, Falkenmark M, Hirsch R, Kundzewicz Z, Lettenmaier D, Stouffer R (2008) Stationarity is dead: Whither water management. Science 319(5863):573–574

Moron V, Vautard R, Ghil M (1998) Trends, interdecadal and interannual oscillations in global sea-surface temperatures. Clim Dyn 14:545–569

Nicholls R, Wong P, Burkett V, Codignotto J, Hay J, McLean R, Ragoonaden S, Woodroffe C (2007) Coastal systems and low-lying areas. In: Solomon S, Qin D, Manning M, Chen Z, Marquis M, Averyt K, Tignor M, Miller H (eds) Climate Change 2007: Impacts, adaptation and vulnerability. Contribution of Working Group II to the Fourth Assessment Report of the Intergovernmental Panel on Climate Change. Cambridge University Press,

Bindoff NL et al. (2007) Observations: oceanic climate change and sea level. In: Solomon S, Qin D, Manning M, Chen Z, Marquis M, Averyt K, Tignor M, Miller H (eds) Climate change 2007: The physical science basis contribution of Working Group I to the fourth assessment report of the Intergovernmental Panel on Climate Change. Cambridge University Press, Cambridge

NOAA (2009) Elevated east coast sea level anomaly: June–July 2009. Technical report NOS CO-OPS 051, NOAA technical report

Osborn TJ (2007) Recent variations in the winter North Atlantic oscillation. Weather 61(12):353–355

Park J, Obeysekera J, Irizarry-Ortiz M, Barnes J, Park-Said W (2010) Climate links and variability of extreme sea-level events at Key West, Pensacola, and Mayport, Florida. J Waterway Port Coast Ocean Eng 136:350

Plaut G, Ghil M, Vautard R (1995) Interannual and interdecadal variability in 335 years of Central England temperature. Science 268:710–713

te Raa L, van Oldenborgh G, Dijkstra H, Philip S (2009) Frequency-dependent effects of the Atlantic meridional overturning on the tropical Pacific Ocean. Ocean Sci Discuss 6:477–490

Ropelewski C, Halpert M (1987) Global and regional scale precipitation patterns associated with the El Niño/Southern oscillation. Mon Wea Rev 115:1606–1626

Ross M, Meeder J, Sah J, Ruiz P, Telesnicki G (2000) The southeast saline everglades revisited: 50 years of coastal vegetation change. J Vegetat Sci 11:101–112

Smith T, Reynolds R, Peterson T, Lawrimore J (2008) Improvements to NOAA's historical merged land-ocean surface temperature analysis (1880–2006). J Climate 21:2283–2296

Speich S, Dijkstra H, Ghil M (1995) Successive bifurcations in a shallow-water model applied to the wind-driven ocean circulation. Nonlinear Proc Geophys 2(3/4):241–268

Sutton R, Hodson D (2007) Climate response to basin-scale warming and cooling of the North Atlantic Ocean. J Clim 20:891–907

Timmermann A, An SI, Krebs U, Goosse H (2005) ENSO suppression due to weakening of the North Atlantic thermohaline circulation. J Clim 18:3122–3139

Timmermann A, Okumura Y, An SI, Clement A, Dong B, Guilyard E, Hu A, Jungclaus J, Renold M, Stocker T, Stouffer R, Sutton R, Xie S, Yin J (2007) The influence of a weakening of the Atlantic meridional overturning circulation on ENSO. J Clim 20:4899–4918

Titus J, Anderson K, Cahoon D, Gesch D, Gill S, Gutierrez B, Thieler E, Williams S (2009) Coastal sensitivity to sea-level rise: a focus on the mid-Atlantic region. Report, US climate change science program and the subcommittee on global change research

Torrence C, Compo GP (1998) A practical guide to wavelet analysis. Bull Am Meteorol Soc 79:61–78

Wakelin S, Woodworth P, Flather R, Williams J (2003) Sea-level dependence on the NAO over the NW European continental shelf. Geophys Res Lett 30(7). doi:10.1029/2003GL017041

Zhang R, Delworth T (2005) Simulated tropical response to a substantial weakening of the Atlantic thermohaline circulation. J Clim 18:1853–1860